Modeling of Multileg Sine-Wave Inverters: A Geometric Approach

Michael J. Ryan, *Member, IEEE*, Robert D. Lorenz, *Fellow, IEEE*, and Rik W. De Doncker, *Senior Member, IEEE*

***Abstract*—Three fundamental sine-wave inverter topologies are analyzed: two-leg (one-phase, two-wire); three-leg (three-phase, three-wire); and four-leg (three-phase, four-wire). The topologies are "full-bridge" voltage-source inverters with LC filters suitable for producing sinusoidal output voltages. The switching states and corresponding output voltage vectors produced by each inverter are identified and presented along with an analysis of the geometric arrangement of these voltage vectors. A pattern of characteristics is established whereby the "qd" modeling forms commonly used with three-leg inverters are extended to address the expanded capabilities of the four-leg inverter. A unique 4×4 decoupling transformation matrix is presented for the four-leg inverter that enables direct transformation between the four-degree-of-freedom (DOF) leg-modulation space of the inverter and its corresponding 3-DOF output-voltage space. This is shown to be directly analogous to the well-known "abc–qd" transformation developed for the three-leg inverter. Fully decoupled models for each inverter are presented.**

***Index Terms*—DC–AC power conversion, inverters, modeling, power electronics, Quad-Transform, uninterruptible power supply.**

I. Introduction

POWER electronic voltage-source inverters (VSI's) with *LC* filters have long been used to synthesize ac voltage, most notably for uninterruptible power supply (UPS) applications where a constant output voltage is supplied to the load. Such sine-wave inverters (SWI's) have been constructed for single-phase and three-phase output. The four-leg inverter has been developed to provide neutral-point control for unbalanced and/or nonlinear three-phase loads [1].

Modeling and control techniques for single-phase (two-leg) SWI's and the three-phase, three-wire (three-leg) SWI's are well established [2]–[5]. Previous analyses of the four-leg SWI have utilized the well-known 3×3 "*abc–qd*" transformation [6] matrix in modeling the operation of the four-leg inverter [7]. While this "*abc–qd*" transformation is widely used for the modeling and control of three-leg inverters, it does not adequately address the extra degree of freedom (DOF) the four-leg inverter provides.

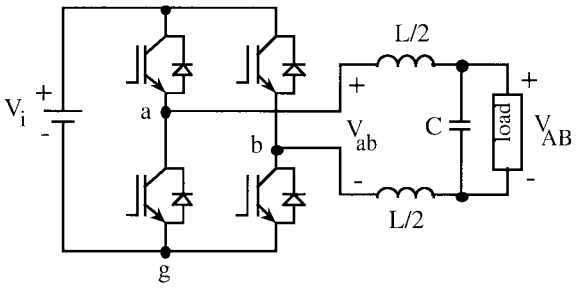

Fig. 1. Two-leg SWI topology.

This paper presents the switching states and output voltage-vectors produced by the two-, three- and four-leg inverters, along with a geometric analysis of the arrangement of these vectors: specifically, how the *leg-voltage vectors project into the output-voltage space*. A pattern of characteristics is established whereby the "*abc–qd*" transformation used with three-leg inverters is extended to address the expanded capabilities of the four-leg inverter. A unique 4×4 decoupling transformation matrix is presented for the four-leg inverter that provides for direct transformation between the 4-DOF leg-modulation space of the inverter and its 3-DOF output-voltage space. With this new "*abcn–qdo*" transformation, the legs of a three-phase, four-wire SWI can be deterministically modulated to produce arbitrary phase voltages, regardless of loading.

II. Two-Leg Inverter

Fig. 1 depicts a two-leg inverter with a simple *LC* output filter. This is the topology commonly used for single-phase SWI's. Each *leg-voltage*, e.g., V_{ag}, can be one of two states, 0 or $+V_i$. The inverter output voltage impressed across the *LC* filter is found simply as

$$V_{ab} = V_{ag} - V_{bg} \quad [\text{V}]. \tag{1}$$

Each leg of a VSI can have one of two possible states: high (1) where the upper switch is on, or low (0) where the lower switch is on. The two-leg inverter produces a total of four (2^2) switching states, depicted in Table I. The corresponding *voltage vectors* are in the last column.

The two inverter legs comprise a 2-DOF system, i.e., each leg can be controlled, or modulated, independently. This can be modeled as *two orthogonal axes*, where each leg-voltage axis ranges from 0 to V_i. This is defined as the *leg-voltage space*

Manuscript received September 17, 1998; revised July 26, 1999. Abstract published on the Internet August 20, 1999.

M. J. Ryan was with the Institute for Power Electronics and Electrical Drives, RWTH-Aachen, 52066 Aachen, Germany. He is now with the Power Controls Program, General Electric Corporate Research and Development Center, Niskayuna, NY 12309 USA (e-mail: ryanm@crd.ge.com).

R. D. Lorenz is with the Department of Electrical and Computer Engineering, University of Wisconsin, Madison, WI 53706 USA (e-mail: lorenz@eceserv0.ece.wisc.edu).

R. W. De Doncker is with the Institute for Power Electronics and Electrical Drives, RWTH-Aachen, 52066 Aachen, Germany (e-mail: dd@isea.rwth-aachen.de).

Publisher Item Identifier S 0278-0046(99)08483-X.

TABLE I
TWO-LEG INVERTER SWITCHING STATES AND VOLTAGE VECTORS

S_a	S_b	V_{ag}	V_{bg}	V_{ab}	Vector #
0	0	0	0	0	**0**
0	1	0	V_i	$-V_i$	**2**
1	0	V_i	0	$+V_i$	**1**
1	1	V_i	V_i	0	**3**

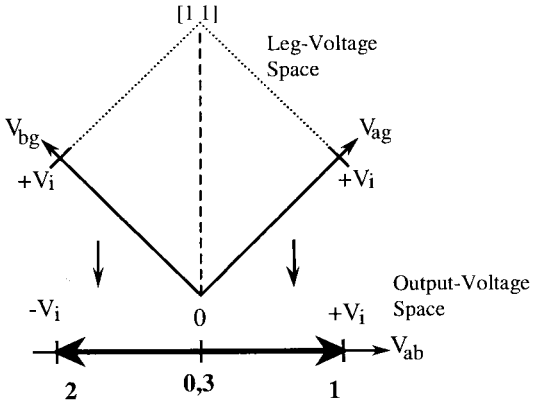

Fig. 2. Projection of leg-voltage space to output-voltage space (two-leg).

of the inverter. The output voltage V_{ab} can be constructed as a *projection* of the leg-voltage space onto a line that is perpendicular to the $[1\ 1]^t$ vector in leg-voltage space. This projection is depicted in Fig. 2. Note that the four corners of the leg-voltage "square" in Fig. 2 represent the four switching states of the two-leg inverter.

In Fig. 2, it can be seen that the leg voltages project into the output-voltage space as *two vectors of equal magnitude equally opposed along a 1-DOF line*. Note that the output-voltage space is spanned by the following two vectors: $\mathbf{1} = [+V_i]$ and $\mathbf{2} = [-V_i]$. These are referred to as the *primary voltage vectors*, as all of the voltage vectors can be formed from combinations of these two. From Table I and Fig. 2, it can be seen that two "zero vectors" are also produced that yield an output voltage of zero: vectors numbered $\mathbf{0}$ and $\mathbf{3}$.

The projection from leg-voltage space to output-voltage space can be represented in mathematical terms by a *transformation matrix*, where the individual leg voltages are transformed into an output voltage and another "placeholder" value, designated V_o, which can be considered a "zero-sequence" voltage

$$\begin{bmatrix} V_{ab} \\ V_o \end{bmatrix} = \begin{bmatrix} 1 & -1 \\ 1 & 1 \end{bmatrix} \begin{bmatrix} V_{ag} \\ V_{bg} \end{bmatrix} \quad \text{or} \quad \begin{bmatrix} V_{ab} \\ V_o \end{bmatrix} = \mathbf{T}_{ab} \begin{bmatrix} V_{ag} \\ V_{bg} \end{bmatrix} \quad [\text{V}]. \tag{2}$$

Note that the placeholder V_o represents the loss of 1 DOF when going from leg-voltage space to output-voltage space. Several points are to be noted about the $\mathbf{T}_{ab}$ matrix.

1) The row and column vectors of $\mathbf{T}_{ab}$ comprise an *orthonormal system*, i.e., the vectors are perpendicular to one another and form a basis for the 2-DOF leg-voltage space. This is proven through the dot product of the vectors: $[1\ -1] \cdot [1\ 1] = 0$, etc.
2) Combinations of $[V_{ag}\ V_{bg}]^t$ parallel to the $[1\ 1]^t$ vector in leg-voltage space (e.g., $[2\ 3]^t$ and $[3\ 4]^t$, etc.) will produce the same output voltage, V_{ab}. Thus, the system is "overdetermined" for producing a given V_{ab}.
3) If the $\mathbf{T}_{ab}$ matrix is represented as

$$\mathbf{T}_{ab} = \begin{bmatrix} \mathbf{a} & \mathbf{b} \\ 1 & 1 \end{bmatrix} \tag{3}$$

the $\mathbf{a} = [1]$ and $\mathbf{b} = [-1]$ column vectors align with the primary voltage vectors, $\mathbf{1}$ and $\mathbf{2}$, respectively, in the output-voltage space, i.e., $\mathbf{1} = \mathbf{a}V_i$, $\mathbf{2} = \mathbf{b}V_i$.

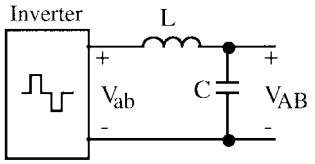

Fig. 3. Two-leg SWI equivalent dynamic model.

Commonly, the legs of the inverter are controlled via pulsewidth modulation (PWM) at a fixed switching frequency. The control of the inverter is then effected by controlling the duty cycle, or modulation, of each leg. While the output-voltage space is only one-dimensional, the 2×2 transform matrix allows modulations for the two legs to be found given a single desired output voltage, V_{ab}, through the inverse of $\mathbf{T}_{ab}$

$$\begin{bmatrix} V_{ag} \\ V_{bg} \end{bmatrix} = [\mathbf{T}_{ab}]^{-1} \begin{bmatrix} V_{ab}^* \\ V_o^* \end{bmatrix} = \begin{bmatrix} \frac{1}{2} & \frac{1}{2} \\ -\frac{1}{2} & \frac{1}{2} \end{bmatrix} \begin{bmatrix} V_{ab}^* \\ V_o^* \end{bmatrix} \quad [\text{V}] \tag{4}$$

where V_o^* is taken as a constant (e.g., $V_o^* = V_i$). Note that modulation strategies, where V_o^* is adjusted to maximize bus voltage utilization, are outside the scope of this paper and will not be discussed. The equivalent dynamic system for the two-leg SWI is shown in Fig. 3, where the inverter output voltage V_{ab} is impressed across the *LC* filter.

In summary, several points are noted for the two-leg inverter.

- The output voltage is found by projecting the leg-voltage space (2 DOF) onto a line (1 DOF) perpendicular to the $[1\ 1]^t$ vector in leg-voltage space. The $[1\ 1]^t$ vector represents the DOF that is lost in going from leg-voltage space to output-voltage space.
- The *two leg voltages project into the output-voltage space as two opposing vectors of equal magnitude in a one-dimensional space (line)*. These are the *primary voltage vectors*, and they are equally arranged in this space, i.e., the sum of the vectors gives the null vector $\mathbf{a} + \mathbf{b} = [0]$.
- The projection from leg-voltage space to output-voltage space is represented by a transformation matrix whose upper column vectors are comprised of the primary vectors, i.e., $[\mathbf{a}\ \mathbf{b}]$.

Similar attributes will be identified for the three-leg inverter in the next section.

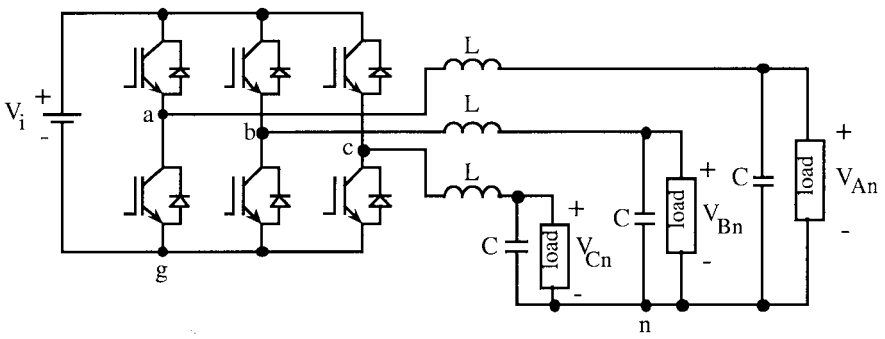

Fig. 4. Three-leg SWI topology.

TABLE II
THREE-LEG INVERTER SWITCHING STATES AND VOLTAGE VECTORS

S_a	S_b	S_c	V_{ag}	V_{bg}	V_{cg}	V_{ng}	V_{an}	V_{bn}	V_{cn}	Vector #
0	0	0	0	0	0	0	0	0	0	**0**
0	0	1	0	0	V_i	$V_i/3$	$-V_i/3$	$-V_i/3$	$2V_i/3$	**5**
0	1	0	0	V_i	0	$V_i/3$	$-V_i/3$	$2V_i/3$	$-V_i/3$	**3**
0	1	1	0	V_i	V_i	$2V_i/3$	$-2V_i/3$	$V_i/3$	$V_i/3$	**4**
1	0	0	V_i	0	0	$V_i/3$	$2V_i/3$	$-V_i/3$	$-V_i/3$	**1**
1	0	1	V_i	0	V_i	$2V_i/3$	$V_i/3$	$-2V_i/3$	$V_i/3$	**6**
1	1	0	V_i	V_i	0	$2V_i/3$	$V_i/3$	$V_i/3$	$-2V_i/3$	**2**
1	1	1	V_i	V_i	V_i	V_i	0	0	0	**7**

III. THREE-LEG INVERTER

Fig. 4 depicts a three-leg inverter connected to a three-phase *LC* filter, with a balanced load. The three-leg inverter can produce only two *independent* output voltages; i.e., if V_{ab} & V_{bc} are known, then V_{ca} is implicitly defined. Thus, three-leg inverters can only produce balanced three-phase voltages (V_{ln}) if the Y-connected load and filter are balanced, where V_{ng} is found as

$$V_{ng} = \frac{(V_{ag} + V_{bg} + V_{cg})}{3} \quad \text{[V]}. \tag{5}$$

The pattern to be noted is that an N-leg inverter with an N-dimensional leg-voltage space can only produce an $(N-1)$-dimensional output-voltage space. From Fig. 4 and (5), the line-to-neutral voltages are found in matrix form as

$$\begin{bmatrix} V_{an} \\ V_{bn} \\ V_{cn} \end{bmatrix} = \frac{1}{3}\begin{bmatrix} 2 & -1 & -1 \\ -1 & 2 & -1 \\ -1 & -1 & 2 \end{bmatrix}\begin{bmatrix} V_{ag} \\ V_{bg} \\ V_{cg} \end{bmatrix} = \mathbf{T}_{ln3}\begin{bmatrix} V_{ag} \\ V_{bg} \\ V_{cg} \end{bmatrix} \quad \text{[V]} \tag{6}$$

where a balanced load is assumed. A three-leg inverter has eight (2^3) possible switching states/voltage vectors, which are listed in Table II.

The three leg voltages $(V_{ag} \;\; V_{bg} \;\; V_{cg})$ of the inverter represent a 3-DOF system that can be depicted as *three orthogonal axes*. The phase voltages $(V_{an} \;\; V_{bn} \;\; V_{cn})$ can be constructed by projecting the 3-DOF leg-voltage space onto a 2-DOF *plane* orthogonal to the $[1 \;\; 1 \;\; 1]^t$ vector in leg-voltage space. This is depicted in Fig. 5, where $V_i = 100$ Vdc is used for convenient scaling.

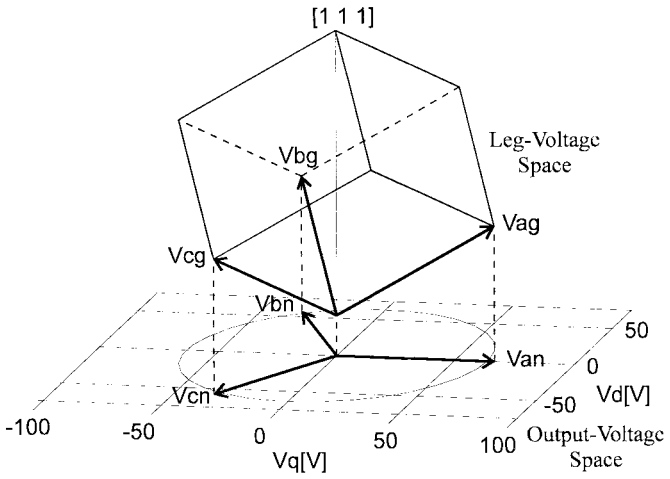

Fig. 5. Leg-voltage space projected onto output-voltage space (three-leg).

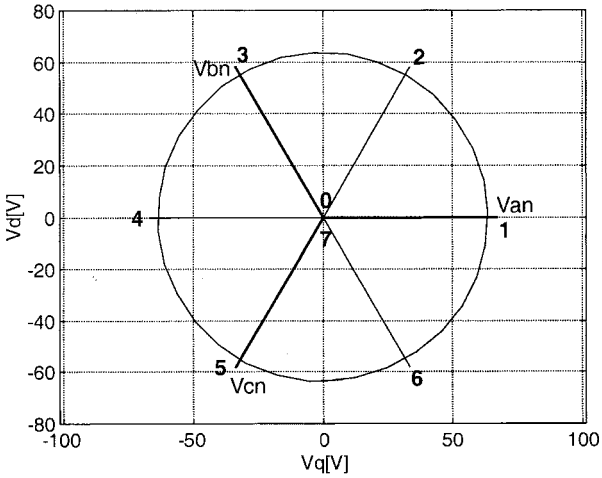

Fig. 6. Three-leg voltage vectors in output-voltage space (qd plane).

From Fig. 5, it can be seen that the leg voltages of the inverter project into the output-voltage space as *three vectors of equal magnitude equally opposed in a 2-DOF plane*. Note the analogy to Fig. 2. The eight corners of the "cube" in Fig. 5 represent the eight switching states/voltage vectors of the three-leg inverter. These voltage vectors project down onto the output-voltage space (plane), as shown in Fig. 6. Note that

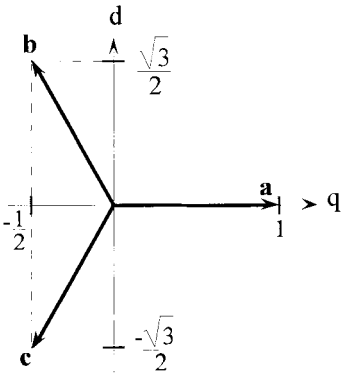

Fig. 7. Three-leg primary voltage vectors in qd plane.

the vectors have been numbered so as to produce a positive-sequence output voltage [6]. Note also from Table II and Fig. 6 that two "zero vectors", **0** and **7**, are again produced. The circle in Figs. 5 and 6 represents balanced three-phase voltage and is shown for reference.

The phase voltages in the qd plane must have their component parts summed to find the "effective" 2-DOF output voltages V_q and V_d. This can be represented with a *transformation matrix*

$$\begin{bmatrix} V_q \\ V_d \\ V_o \end{bmatrix} = \frac{2}{3}\begin{bmatrix} 1 & -\frac{1}{2} & -\frac{1}{2} \\ 0 & \frac{\sqrt{3}}{2} & -\frac{\sqrt{3}}{2} \\ \frac{1}{\sqrt{2}} & \frac{1}{\sqrt{2}} & \frac{1}{\sqrt{2}} \end{bmatrix}\begin{bmatrix} V_{an} \\ V_{bn} \\ V_{cn} \end{bmatrix} = \mathbf{T}_{qdo}\begin{bmatrix} V_{an} \\ V_{bn} \\ V_{cn} \end{bmatrix} \quad \text{[V]}. \tag{7}$$

This is often referred to as the amplitude-invariant "qd" transformation [6]. The V_o or "zero-sequence" axis is used as a placeholder so that a square 3×3 matrix is developed and, as with the two-leg inverter, represents the loss of 1 DOF when going from leg-voltage space to output-voltage space.

Points to note about the $\mathbf{T}_{qdo}$ matrix are the following.

1) The row and column vectors are orthonormal and form a basis for the 3-DOF leg-voltage space.
2) Combinations of $[V_{ag}\ V_{bg}\ V_{cg}]^t$ parallel to the $[1\ 1\ 1]^t$ vector in leg-voltage space (e.g., $[2\ 3\ 1]^t$ and $[3\ 4\ 2]^t$) will produce the same output voltage, $[V_{an}\ V_{bn}\ V_{cn}]^t$.
3) Representing the $\mathbf{T}_{qdo}$ matrix as

$$\mathbf{T}_{qdo} = \frac{2}{3}\begin{bmatrix} \mathbf{a} & \mathbf{b} & \mathbf{c} \\ \frac{1}{\sqrt{2}} & \frac{1}{\sqrt{2}} & \frac{1}{\sqrt{2}} \end{bmatrix} \tag{8}$$

the **a**, **b**, and **c** column vectors are of equal magnitude and align with the phase-voltage vectors in the qd plane. These are the *primary voltage vectors* of the system, and are depicted in Fig. 7.

Note in Fig. 7 that the $[\mathbf{a}\ \mathbf{b}\ \mathbf{c}]$ vectors align with the $[\mathbf{1}\ \mathbf{3}\ \mathbf{5}]$ voltage vectors in Fig. 6. All eight voltage vectors of the three-leg inverter are found as combinations of the primary voltage vectors, e.g.,

$$\mathbf{1}+\mathbf{3} = \left[\left(\frac{2}{3}V_i\right)\mathbf{a}\right] + \left[\left(\frac{2}{3}V_i\right)\mathbf{b}\right] = \left(\frac{2}{3}V_i\right)\begin{bmatrix} \frac{1}{2} \\ \frac{\sqrt{3}}{2} \end{bmatrix} = \mathbf{2} \quad \text{[V]}. \tag{9}$$

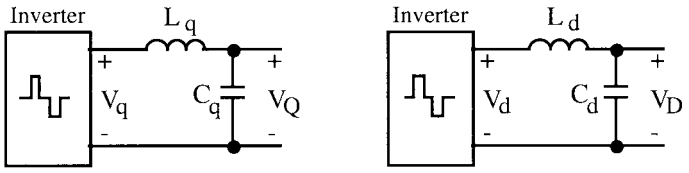

Fig. 8. Three-leg SWI equivalent dynamic model.

Combining (6) and (7), the full transformation from leg-voltage space to qd space is found

$$\begin{bmatrix} V_q \\ V_d \\ V_o \end{bmatrix} = \mathbf{T}_{qdo}\mathbf{T}_{ln3}\begin{bmatrix} V_{ag} \\ V_{bg} \\ V_{cg} \end{bmatrix} = \frac{2}{3}\begin{bmatrix} 1 & -\frac{1}{2} & -\frac{1}{2} \\ 0 & \frac{\sqrt{3}}{2} & -\frac{\sqrt{3}}{2} \\ 0 & 0 & 0 \end{bmatrix}\begin{bmatrix} V_{ag} \\ V_{bg} \\ V_{cg} \end{bmatrix} = \mathbf{T}_{lg3}\begin{bmatrix} V_{ag} \\ V_{bg} \\ V_{cg} \end{bmatrix} \quad \text{[V]}. \tag{10}$$

Note that, as the three-leg inverter has only a 2-DOF output-voltage space, no zero-sequence voltage V_o is formed. The upper column vectors of the $\mathbf{T}_{lg3}$ transform are again comprised of the three primary voltage vectors. Thus, as depicted in Fig. 5, the three leg voltages are projected into the output-voltage space along three opposing vectors equally arranged in a plane. As was done for the two-leg inverter, the inverse of the $\mathbf{T}_{qdo}$ matrix can be used to find leg modulation values from the desired $[V_q\ V_d\ V_o]^t$ values

$$\begin{bmatrix} V_{ag} \\ V_{bg} \\ V_{cg} \end{bmatrix} = [\mathbf{T}_{qdo}]^{-1}\begin{bmatrix} V_q^* \\ V_d^* \\ V_o^* \end{bmatrix} = \begin{bmatrix} 1 & 0 & \frac{1}{\sqrt{2}} \\ -\frac{1}{2} & \frac{\sqrt{3}}{2} & \frac{1}{\sqrt{2}} \\ -\frac{1}{2} & -\frac{\sqrt{3}}{2} & \frac{1}{\sqrt{2}} \end{bmatrix}\begin{bmatrix} V_q^* \\ V_d^* \\ V_o^* \end{bmatrix} \quad \text{[V]}. \tag{11}$$

This can be verified with (10)

$$\begin{bmatrix} V_q \\ V_d \\ V_o \end{bmatrix} = \mathbf{T}_{qdo}\mathbf{T}_{ln3}[\mathbf{T}_{qdo}]^{-1}\begin{bmatrix} V_q^* \\ V_d^* \\ V_o^* \end{bmatrix} = \begin{bmatrix} 1 & 0 & 0 \\ 0 & 1 & 0 \\ 0 & 0 & 0 \end{bmatrix}\begin{bmatrix} V_q^* \\ V_d^* \\ V_o^* \end{bmatrix} \quad \text{[V]}. \tag{12}$$

As can be seen in (12), the desired $[V_q\ V_d]^t$ output is formed. Because the $\mathbf{T}_{qdo}$ transform decouples the three phase voltages into their equivalent 2-DOF components, the three-leg inverter can now be reduced to two *independent* single-phase circuits, as shown in Fig. 8.

In Fig. 8, the filter components are equal to the original components $L_q = L_d = L$, $C_q = C_d = C$. Thus, as is widely

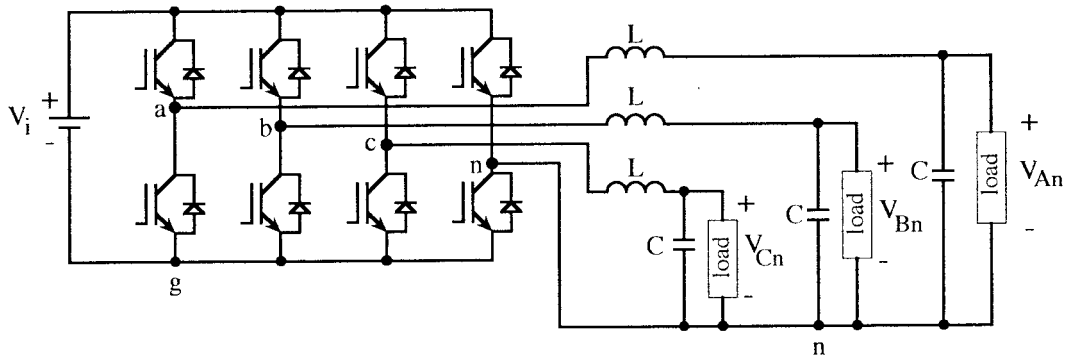

Fig. 9. Four-leg SWI topology.

used, the $\mathbf{T}_{qdo}$ transformation allows the two output axes of the three-leg inverter to be controlled independently.

In summary, several points are noted about the three-leg inverter.

- The output voltage is found by projecting the leg-voltage space (3 DOF) onto a plane (2 DOF) perpendicular to the $[1\ 1\ 1]^t$ vector in leg-voltage space, where the $[1\ 1\ 1]^t$ vector again represents the redundant axis (i.e., loss of 1 DOF).
- The *three leg voltages project into the output-voltage space as three opposing vectors of equal magnitude in a two-dimensional space (plane)*. These are the *primary voltage vectors*, and they are equally arranged in this space, i.e., the sum of the vectors gives the null vector $\mathbf{a}+\mathbf{b}+\mathbf{c}=[0\ 0]^t$.
- The projection from leg-voltage space to output-voltage space is represented by a transformation matrix whose upper column vectors are comprised of the primary vectors, i.e., $[\mathbf{a}\ \mathbf{b}\ \mathbf{c}]$.

A pattern of characteristics has now been identified that guides the analysis and modeling of the four-leg inverter presented in the next section.

IV. Four-Leg Inverter

Fig. 9 depicts a four-leg inverter connected to a three-phase *LC* filter with arbitrary loads. The fourth leg controls the neutral voltage and conducts any neutral currents. Through this, the four-leg inverter can produce *three independent output voltages*, regardless of load. The line-to-neutral voltages are found from Fig. 9 as

$$\begin{bmatrix} V_{an} \\ V_{bn} \\ V_{cn} \\ V_n \end{bmatrix} = \begin{bmatrix} 1 & 0 & 0 & -1 \\ 0 & 1 & 0 & -1 \\ 0 & 0 & 1 & -1 \\ 0 & 0 & 0 & 0 \end{bmatrix} \begin{bmatrix} V_{ag} \\ V_{bg} \\ V_{cg} \\ V_{ng} \end{bmatrix} = \mathbf{T}_{ln4} \begin{bmatrix} V_{ag} \\ V_{bg} \\ V_{cg} \\ V_{ng} \end{bmatrix} \quad [\text{V}] \tag{13}$$

where a placeholder V_n has been defined to form a 4×4 transform. Note that this placeholder value again represents the loss of 1 DOF in going from leg-voltage space to output-voltage space, and has no bearing on the actual output voltages produced. A four-leg inverter has 16 (2^4) possible switching states/voltage vectors, given in Table III. Note that the voltage vectors in Table III have been numbered by the "binary order" of the switching states and not with respect to a switching pattern, as is done with the three-leg inverter [6].

TABLE III
Four-Leg Inverter Switching States and Voltage Vectors

S_a	S_b	S_c	S_d	V_{ag}	V_{bg}	V_{cg}	V_{ng}	V_{an}	V_{bn}	V_{cn}	Vector #
0	0	0	0	0	0	0	0	0	0	0	**0**
0	0	0	1	0	0	0	V_i	$-V_i$	$-V_i$	$-V_i$	**1**
0	0	1	0	0	0	V_i	0	0	0	V_i	**2**
0	0	1	1	0	0	V_i	V_i	$-V_i$	$-V_i$	0	**3**
0	1	0	0	0	V_i	0	0	0	V_i	0	**4**
0	1	0	1	0	V_i	0	V_i	$-V_i$	0	$-V_i$	**5**
0	1	1	0	0	V_i	V_i	0	0	V_i	V_i	**6**
0	1	1	1	0	V_i	V_i	V_i	$-V_i$	0	0	**7**
1	0	0	0	V_i	0	0	0	V_i	0	0	**8**
1	0	0	1	V_i	0	0	V_i	0	$-V_i$	$-V_i$	**9**
1	0	1	0	V_i	0	V_i	0	V_i	0	V_i	**10**
1	0	1	1	V_i	0	V_i	V_i	0	$-V_i$	0	**11**
1	1	0	0	V_i	V_i	0	0	V_i	V_i	0	**12**
1	1	0	1	V_i	V_i	0	V_i	0	0	$-V_i$	**13**
1	1	1	0	V_i	V_i	V_i	0	V_i	V_i	V_i	**14**
1	1	1	1	V_i	V_i	V_i	V_i	0	0	0	**15**

The four leg voltages ($V_{ag}\ V_{bg}\ V_{cg}\ V_{ng}$) can be depicted as *four orthogonal axes*, whereby the output phase voltages can be constructed by projecting this 4-DOF leg-voltage space into a 3-DOF output-voltage space orthogonal to the $[1\ 1\ 1\ 1]^t$ vector in leg-voltage space. In constructing this projection, the pattern identified with the two-leg and three-leg inverters is followed: the leg voltages of an N-leg inverter project into the output-voltage space along N vectors of equal magnitude equally arranged in an $(N-1)$-DOF space.

Thus, the four leg voltages of the four-leg inverter should project into the 3-DOF output space along four vectors of equal magnitude equally arranged in a 3-DOF space. This arrangement is depicted in Fig. 10, where the three primary voltage vectors of Fig. 7 have been augmented with an additional vector $\mathbf{n}$.

Note in Fig. 10 that the o axis now represents another DOF, and not just a placeholder value (the circle in Fig. 10 again represents the path of balanced three-phase voltage in the qd plane). The $[\mathbf{a}\ \mathbf{b}\ \mathbf{c}\ \mathbf{n}]$ vectors in Fig. 10 form the corners of a symmetrical tetrahedron and, as was recognized for the

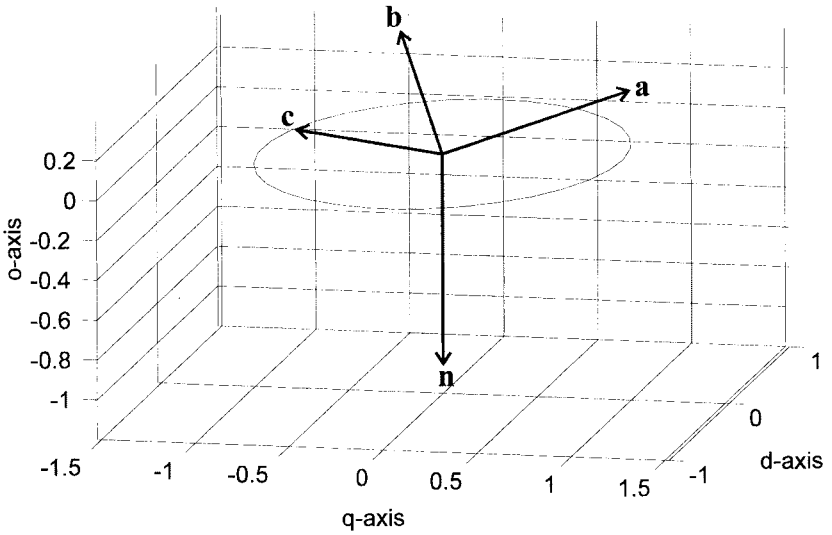

Fig. 10. Four-leg primary voltage vectors in qdo space.

two-leg and three-leg inverters, these vectors sum to zero

$$\mathbf{a}+\mathbf{b}+\mathbf{c}+\mathbf{n} = \begin{bmatrix} 1 \\ 0 \\ \frac{1}{2\sqrt{2}} \end{bmatrix} + \begin{bmatrix} -\frac{1}{2} \\ \frac{\sqrt{3}}{2} \\ \frac{1}{2\sqrt{2}} \end{bmatrix} + \begin{bmatrix} -\frac{1}{2} \\ -\frac{\sqrt{3}}{2} \\ \frac{1}{2\sqrt{2}} \end{bmatrix} + \begin{bmatrix} 0 \\ 0 \\ -\frac{3}{2\sqrt{2}} \end{bmatrix} = \begin{bmatrix} 0 \\ 0 \\ 0 \end{bmatrix}. \tag{14}$$

These *primary voltage vectors* can then be used to form a 4×4 *transformation matrix* from phase-voltage space to a new "qdo" space by using $[\mathbf{a}\ \mathbf{b}\ \mathbf{c}\ \mathbf{n}]$ as the upper part of the new matrix $\mathbf{T}_{qdoz}$

$$\mathbf{T}_{qdoz} = \frac{2}{3}\begin{bmatrix} \mathbf{a} & \mathbf{b} & \mathbf{c} & \mathbf{n} \\ \frac{\sqrt{3}}{2\sqrt{2}} & \frac{\sqrt{3}}{2\sqrt{2}} & \frac{\sqrt{3}}{2\sqrt{2}} & \frac{\sqrt{3}}{2\sqrt{2}} \end{bmatrix}. \tag{15}$$

The bottom row of $\mathbf{T}_{qdoz}$ is found by "completing the square," where the row and column vectors are formed to be orthonormal. As with the two- and three-leg inverters, the $\mathbf{T}_{qdoz}$ matrix transforms phase-voltage space into an equivalent *orthonormal* 3-DOF output-voltage space

$$\begin{bmatrix} V_q \\ V_d \\ V_o \\ V_z \end{bmatrix} = \frac{2}{3}\begin{bmatrix} 1 & -\frac{1}{2} & -\frac{1}{2} & 0 \\ 0 & \frac{\sqrt{3}}{2} & -\frac{\sqrt{3}}{2} & 0 \\ \frac{1}{2\sqrt{2}} & \frac{1}{2\sqrt{2}} & \frac{1}{2\sqrt{2}} & -\frac{3}{2\sqrt{2}} \\ \frac{\sqrt{3}}{2\sqrt{2}} & \frac{\sqrt{3}}{2\sqrt{2}} & \frac{\sqrt{3}}{2\sqrt{2}} & \frac{\sqrt{3}}{2\sqrt{2}} \end{bmatrix}\begin{bmatrix} V_{an} \\ V_{bn} \\ V_{cn} \\ V_n \end{bmatrix} = \mathbf{T}_{qdoz}\begin{bmatrix} V_{an} \\ V_{bn} \\ V_{cn} \\ V_n \end{bmatrix} \quad [\text{V}] \tag{16}$$

where the term V_z is defined as a placeholder (for the loss of 1 DOF). This new transform is referred to as the *Quad-Transform*. Points to note about the $\mathbf{T}_{qdoz}$ matrix are as follows.

1) The $\mathbf{T}_{qdoz}$ matrix is orthonormal and, hence, invertible, and the row and column vectors form a basis for the 4-DOF leg-voltage space.
2) Combinations of $[V_{ag}\ V_{bg}\ V_{cg}\ V_{ng}]^t$ parallel to the $[1\ 1\ 1\ 1]^t$ vector in leg-voltage space (e.g., $[2\ 3\ 1\ 4]^t$ & $[3\ 4\ 2\ 5]^t$) will produce the same output voltage.
3) The "qd" quantities defined for the three-leg inverter in (7) have been preserved in $\mathbf{T}_{qdoz}$.
4) The scale of V_o in (16) is 1/2 of what is defined in (7) for the three-leg inverter.

Using (13) and (16), the complete transformation from leg-voltage space to output-voltage space can be formed

$$\begin{bmatrix} V_q \\ V_d \\ V_o \\ V_z \end{bmatrix} = \mathbf{T}_{qdoz}\mathbf{T}_{ln4}\begin{bmatrix} V_{ag} \\ V_{bg} \\ V_{cg} \\ V_{ng} \end{bmatrix} = \frac{2}{3}\begin{bmatrix} 1 & -\frac{1}{2} & -\frac{1}{2} & 0 \\ 0 & \frac{\sqrt{3}}{2} & -\frac{\sqrt{3}}{2} & 0 \\ \frac{1}{2\sqrt{2}} & \frac{1}{2\sqrt{2}} & \frac{1}{2\sqrt{2}} & -\frac{3}{2\sqrt{2}} \\ \frac{\sqrt{3}}{2\sqrt{2}} & \frac{\sqrt{3}}{2\sqrt{2}} & \frac{\sqrt{3}}{2\sqrt{2}} & -\frac{3\sqrt{3}}{2\sqrt{2}} \end{bmatrix}\begin{bmatrix} V_{ag} \\ V_{bg} \\ V_{cg} \\ V_{ng} \end{bmatrix}$$
$$= \frac{2}{3}\begin{bmatrix} \mathbf{a} & \mathbf{b} & \mathbf{c} & \mathbf{n} \\ \frac{\sqrt{3}}{2\sqrt{2}} & \frac{\sqrt{3}}{2\sqrt{2}} & \frac{\sqrt{3}}{2\sqrt{2}} & -\frac{3\sqrt{3}}{2\sqrt{2}} \end{bmatrix}\begin{bmatrix} V_{ag} \\ V_{bg} \\ V_{cg} \\ V_{ng} \end{bmatrix}$$
$$= \mathbf{T}_{lg4}\begin{bmatrix} V_{ag} \\ V_{bg} \\ V_{cg} \\ V_{ng} \end{bmatrix} \quad [\text{V}]. \tag{17}$$

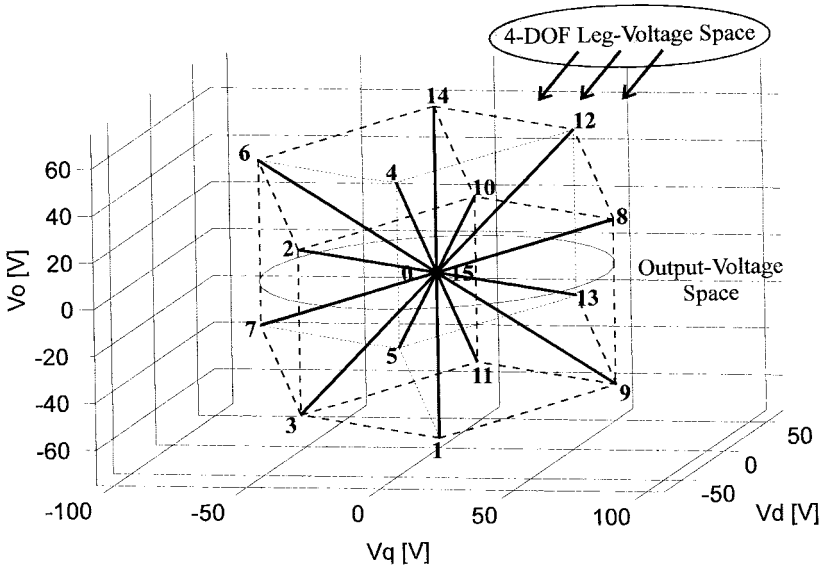

Fig. 11. Four-leg voltage vectors in qdo space ($V_i = 100$ Vdc).

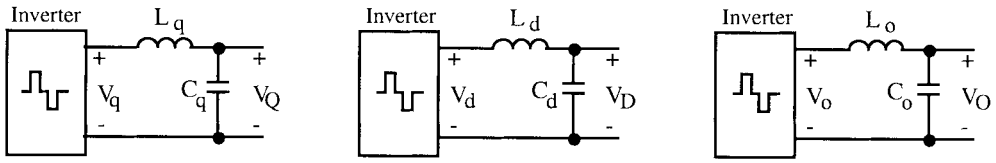

Fig. 12. Equivalent "qdo" dynamic model of the four-leg inverter.

Note in (17) that the neutral leg voltage V_{ng} only affects the "zero-sequence" voltage V_o. Note additionally that the upper column vectors of $\mathbf{T}_{lg4}$ are again composed of the four primary voltage vectors. Thus, as was desired, the four leg voltages are projected into the output-voltage space along four opposing vectors equally arranged in a 3-DOF space. Using (17), the 16 voltage vectors of the four-leg inverter (Table III) are transformed into the new "qdo" output-voltage space, and are shown in Fig. 11 ($V_i = 100$ Vdc is again used for convenient scaling).

In Fig. 11, it can be seen that the voltage vectors fill out a "sphere" in qdo space, analogous to the "circle" in Fig. 6. Note in Table III and Fig. 11 that two zero vectors, $\mathbf{0}$ and $\mathbf{15}$, are again produced. Note also that the primary vectors $[\mathbf{a}\ \mathbf{b}\ \mathbf{c}\ \mathbf{n}]$ in Fig. 10 align with $[\mathbf{8}\ \mathbf{4}\ \mathbf{2}\ \mathbf{1}]$ in Fig. 11. All 16 voltage vectors of the four-leg inverter are found as combinations of the primary voltage vectors, e.g.,

$$\mathbf{8}+\mathbf{4} = \left[\left(\frac{2}{3}V_i\right)\mathbf{a}\right] + \left[\left(\frac{2}{3}V_i\right)b\right] = \left(\frac{2}{3}V_i\right)\begin{bmatrix}\frac{1}{2}\\ \frac{\sqrt{3}}{2}\\ \frac{1}{\sqrt{2}}\end{bmatrix} = \mathbf{12} \quad [\text{V}]. \tag{18}$$

As was depicted for the two-leg and three-leg inverters, the inverse of $\mathbf{T}_{qdoz}$ can be used to find four leg-modulation values from desired output values

$$\begin{bmatrix}V_{ag}\\ V_{bg}\\ V_{cg}\\ V_{ng}\end{bmatrix} = [\mathbf{T}_{qdoz}]^{-1}\begin{bmatrix}V_q^*\\ V_d^*\\ V_o^*\\ V_z^*\end{bmatrix} = \begin{bmatrix}1 & 0 & \frac{1}{2\sqrt{2}} & \frac{\sqrt{3}}{2\sqrt{2}}\\ -\frac{1}{2} & \frac{\sqrt{3}}{2} & \frac{1}{2\sqrt{2}} & \frac{\sqrt{3}}{2\sqrt{2}}\\ -\frac{1}{2} & -\frac{\sqrt{3}}{2} & \frac{1}{2\sqrt{2}} & \frac{\sqrt{3}}{2\sqrt{2}}\\ 0 & 0 & -\frac{3}{2\sqrt{2}} & \frac{\sqrt{3}}{2\sqrt{2}}\end{bmatrix}\begin{bmatrix}V_q^*\\ V_d^*\\ V_o^*\\ V_z^*\end{bmatrix} \quad [\text{V}]. \tag{19}$$

This can be verified with (17)

$$\begin{bmatrix}V_q\\ V_d\\ V_o\\ V_z\end{bmatrix} = \mathbf{T}_{qdoz}\mathbf{T}_{ln4}[\mathbf{T}_{qdoz}]^{-1}\begin{bmatrix}V_q^*\\ V_d^*\\ V_o^*\\ V_z^*\end{bmatrix} = \begin{bmatrix}1 & 0 & 0 & 0\\ 0 & 1 & 0 & 0\\ 0 & 0 & 1 & 0\\ 0 & 0 & \sqrt{3} & 0\end{bmatrix}\begin{bmatrix}V_q^*\\ V_d^*\\ V_o^*\\ V_z^*\end{bmatrix} \quad [\text{V}]. \tag{20}$$

Thus, the desired output voltages are produced, excepting V_z which is only a mathematical fabrication. Since the operation of the four-leg inverter has now been reduced to three

orthogonal output voltages, the four-leg SWI can now be modeled as three *independent* single-phase circuits, as shown in Fig. 12. Note in Fig. 12 that the filter components are again equal to the original components: $L_q = L_d = L_o = L$, $C_q = C_d = C_o = C$.

As Fig. 12 depicts, the $\mathbf{T}_{qdoz}$ transformation enables the three output axes of the four-leg inverter to be controlled independently, thus providing full control of $[V_q\ V_d\ V_o]^t$. This new Quad-Transform has been successfully used to control a prototype four-leg SWI; details and experimental results can be found in [1] and [8].

V. Conclusion

Three SWI topologies have been analyzed: a two-leg (single-phase, two-wire), a three-leg (three-phase, three-wire), and a four-leg (three-phase, four-wire). The switching states/voltage vectors of each topology have been identified and presented along with an analysis of the geometric arrangement of these voltage vectors. Several conclusions are drawn.

- An N-leg inverter has an N-dimensional leg-voltage space, but only controls an $(N-1)$-dimensional output-voltage space. The leg voltages of an N-leg inverter project into the output-voltage space along N vectors of equal magnitude equally arranged in an $(N-1)$-DOF space. These are defined as the *primary voltages vectors*.
- The projection from leg-voltage space to output-voltage space can be represented by an $N \times N$ *transformation matrix*. The upper column vectors of this matrix are comprised of the primary voltage vectors. The transformation matrix is invertible, and the inverse can be used to find N leg modulations from $(N-1)$ desired output voltages.
- The output-voltage space of the inverters consists of orthogonal axes and, thus, the effective $(N-1)$ output voltages of an N-leg inverter are decoupled, and can be controlled independently.
- A unique 4×4 "*abcn–qdo*" transformation matrix has been presented for the four-leg inverter that enables fully decoupled control of its 3-DOF output-voltage space. This new matrix is called the Quad-Transform.

References

[1] M. J. Ryan, "Analysis, modeling and control of three-phase, four-wire sine wave inverter systems," Ph.D. dissertation, Elect. Comput. Eng. Dep., Univ. Wisconsin, Madison, 1997.

[2] M. J. Ryan, W. E. Brumsickle, and R. D. Lorenz, "Control topology options for single phase UPS inverters," *IEEE Trans. Ind. Applicat.*, vol. 33, pp. 493–501, Mar./Apr. 1997.

[3] R. W. De Doncker and J. P. Lyons, "Control of three phase power supplies for ultra low THD," in *Proc. IEEE APEC'91*, 1991, pp. 622–629.

[4] Y. Miguchi, A. Kawamura, and R. Hoft, "Decoupling servo-control of three-phase PWM inverter for UPS application," in *Conf. Rec. IEEE-IAS Annu. Meeting*, 1987, pp. 724–733.

[5] N. Abdel-Rahim and J. E. Quaicoe, "Three-phase voltage-source UPS inverter with voltage-controlled current-regulated feedback control scheme," in *Proc. IEEE IECON'94*, 1994, pp. 497–502.

[6] D. W. Novotny and T. A. Lipo, *Vector Control and Dynamics of AC Drives*. Oxford, U.K.: Oxford Univ. Press, 1997.

[7] V. H. Prasad, D. Boroyevich, and R. Zhang, "Analysis and comparison of space vector modulation schemes for a four-leg voltage source inverter," in *Proc. IEEE APEC'97*, 1997, pp. 864–871.

[8] M. J. Ryan, R. W. De Doncker, and R. D. Lorenz, "Decoupled control of a four-leg inverter via a new 4×4 transformation matrix," in *Proc. IEEE PESC'99*, 1999, pp. 187–192.

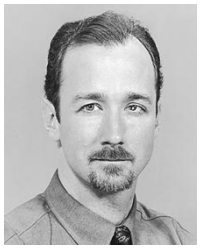

Michael J. Ryan (S'92–M'92) received the B.S. degree from the University of Connecticut, Storrs, the M.E. degree from Rensselaer Polytechnic Institute, Troy, NY, and the Ph.D. degree from the University of Wisconsin, Madison, in 1988, 1992, and 1997, respectively, all in electrical engineering.

His Ph.D. research focused on power electronic inverters and their control. Following receipt of the Ph.D. degree, he engaged in post-doctoral research on induction heating at the Institute for Power Electronics and Electric Drives, RWTH-Aachen, Aachen, Germany. He is currently with the Power Controls Program, General Electric Corporate Research and Development Center, Schenectady, NY. He has had a wide range of industrial experience, including positions at General Electric, Hamilton Standard, and Otis Elevator. His work has included: power electronic converters for brush and brushless dc motors; real-time microprocessor control and programming; path planning, kinematics, and control for multi-axis winding machines; and soft-switching design of resonant inverters for ac traction motor applications. While at the University of Wisconsin, he worked in the Wisconsin Power Electronics Research Center (WisPERC) on projects including dc–dc converters, variable-speed generation systems, and UPS inverter control. In addition, he worked with the university's Hybrid Electric Vehicle Group on vehicles that won first-place titles at several national competitions.

Dr. Ryan is a member of the IEEE Industry Applications Society.

Robert D. Lorenz (S'83–M'84–SM'91–F'98) received the B.S., M.S., and Ph.D. degrees from the University of Wisconsin, Madison, in 1969, 1970, and 1984 respectively.

Since 1984, he has been a member of the faculty of the University of Wisconsin, Madison, where he is the Consolidated Papers Foundation Professor of Controls Engineering in the Mechanical Engineering and in the Electrical and Computer Engineering Departments. He is also Co-Director of the Wisconsin Electric Machines and Power Electronics Consortium. He was a Visiting Research Professor in the Electrical Drives Group, Catholic University of Leuven, Leuven, Belgium, in 1989 and in the Power Electronics and Electrical Drives Institute, Technical University of Aachen, Aachen, Germany, in the summers of 1987, 1991, 1995, 1997, and 1999. In 1969–1970, he conducted Master thesis research at the Technical University of Aachen. From 1972 to 1982, he was a member of the Research Staff at the Gleason Works, Rochester, NY. His current research interests include sensorless electromagnetic motor/actuator technologies, real-time signal processing and estimation techniques, precision multi-axis motion control, and ac drive and high-precision machine control technologies.

Dr. Lorenz is currently the Secretary of the IEEE Industry Applications Society (IAS) and immediate past Chair of the IAS Awards Department. He is also past Chairman of the IAS Industrial Drives Committee and is a member of the IAS Electric Machines, Industrial Power Converter, and Industrial Automation and Control Committees. He is a Registered Professional Engineer in the States of New York and Wisconsin. He is also a member of the American Society of Mechanical Engineers, Instrument Society of America, and Society of Photo-Optical Instrumentation Engineers.

Rik W. De Doncker (M'87–SM'99) received the B.S. and M.S. degrees and the Ph.D. degree (*summa cum laude*) in electrical engineering from the Katholieke Universiteit Leuven, Leuven, Belgium in 1978, 1981, and 1986 respectively.

In 1987, he was appointed a Visiting Associate Professor at the University of Wisconsin, Madison, where he lectured and conducted research on field-oriented controllers for high-performance induction motor drives. In 1988, he was a General Electric Company Fellow in the microelectronic center, IMEC, Leuven, Belgium. In December 1988, he joined the General Electric Company Corporate Research and Development Center, Schenectady, NY, where he led research on drives and high-power soft-switching converters, ranging from 100 kW to 4 MW, for aerospace, industrial, and traction applications. In 1994, he joined Silicon Power Corporation (formerly GE-SPCO) as Vice President, Technology. He worked on high-power converter systems and MTO devices and was responsible for the development and production of a 15-kV medium-voltage transfer switch. Since October 1996, he has been a Professor at RWTH-Aachen, Aachen, Germany, where he leads the Institute for Power Electronics and Electrical Drives. He has published over 45 technical papers and is the holder of 18 patents, with several pending.

Dr. De Doncker is an active member of the IEEE Industry Applications Society (IAS) Industrial Drives Committee and Chairman of the IAS Industrial Power Converter Committee. He is the founding Chairman of the German IEEE IAS-PELS Joint Chapter. He is also the recipient of two IAS Prize Paper Awards.